Osteoarthritis and Cartilage Open 6 (2024) 100528

Contents lists available at ScienceDirect

Osteoarthritis and Cartilage Open

journal homepage: www.elsevier.com/journals/osteoarthritis-and-cartilage-open/2665-9131

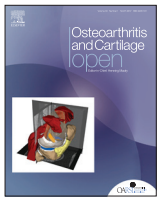

TNFα has differential effects on the transcriptome profile of selected populations in murine cartilage

Ernesto Canalis [a,b,c,*], Lauren Schilling [c], Emily Denker [c]

[a] Departments of Orthopaedic Surgery, UConn Health, Farmington, CT 06030, USA
[b] Departments of Medicine, UConn Health, Farmington, CT 06030, USA
[c] UConn Musculoskeletal Institute, UConn Health, Farmington, CT 06030, USA

ARTICLE INFO

Handling Editor: Professor H Madry

Keywords:
TNFα
Chondrocytes
Inflammation
Transcriptome
IGF1
IGF2

ABSTRACT

Objective: To further our understanding of the role of tumor necrosis factor (TNF)α on the inflammatory response in chondrocytes.
Design: We explored the effects of TNFα on the transcriptome of epiphyseal chondrocytes from newborn C57BL/6 mice at the total and single cell (sc) resolution.
Results: Gene set enrichment analysis of total RNA-Seq from TNFα-treated chondrocytes revealed enhanced response to biotic stimulus, defense and immune response and cytokine signaling and suppressed cartilage and skeletal morphogenesis and development. scRNA-Seq analyzed 14,239 cells and 24,320 genes and distinguished 16 cell clusters. The more prevalent ones were constituted by limb bud and chondrogenic cells and fibroblasts comprising ~73 % of the cell population. Genes expressed by joint fibroblasts were detected in 5 clusters comprising ~45 % of the cells isolated. Pseudotime trajectory finding revealed an association between fibroblast and chondrogenic clusters which was not modified by TNFα. TNFα decreased the total cells recovered by 18.5 % and the chondrogenic, limb bud and mesenchymal clusters by 32 %, 27 % and 7 %, respectively. TNFα had profound effects on the insulin-like growth factor (IGF) axis decreasing *Igf1*, *Igf2* and *Igfbp4* and inducing *Igfbp3* and *Igfbp5*, explaining an inhibition of collagen biosynthesis, cartilage and skeletal morphogenesis. Ingenuity Pathway Analysis of scRNA-Seq data revealed that TNFα enhanced the osteoarthritis, rheumatoid arthritis, pathogen induced cytokine storm and interleukin 6 signaling pathways and suppressed fibroblast growth factor signaling.
Conclusions: Epiphyseal chondrocytes are constituted by diverse cell populations distinctly regulated by TNFα to promote inflammation and suppression of matrix biosynthesis and growth.

1. Introduction

Osteoarthritis is a chronic inflammatory and degenerative disease of the joint affecting the cartilage, synovium and subchondral bone [1–3]. Although there is a degenerative component to osteoarthritis, the disease is a complex disorder affecting the joint and driven by a host of proinflammatory signals, including tumor necrosis factor α (TNFα) [4–7]. These are often released by macrophages and immune cells infiltrating the synovium although articular chondrocytes also are a source of inflammatory molecules that contribute to the pathogenesis of the disease [4,6].

The excessive release of TNFα, interleukin (IL)6 and IL1β during inflammation perturbs joint homeostasis, promotes pathologic bone erosion and is mechanistically relevant to the development of the disease. Recently, we demonstrated that NOTCH2, one of the four Notch receptors, sensitizes osteoclasts to the effect of TNFα on bone resorption and enhances the inflammatory response to TNFα in epiphyseal chondrocytes as well as the pathways associated with inflammation and the phagosome [8,9]. However, the mechanisms responsible and the cells affected by TNFα were not pursued. This is necessary to have a better understanding of the effects of TNFα and its interactions with other signals in the joint environment.

Abbreviations: DMEM, Dulbecco's modified Eagle's medium; ES, enrichment scores; FBS, fetal bovine serum; FDR, false discovery rate; FGF, fibroblast growth factor; GEO, Gene Expression Omnibus; GSEA, Gene Set Enrichment Analysis; IPA, ingenuity pathway analysis; IGF, insulin-like growth factor; IGFBP, IGF binding protein; MMP, metalloproteinases; NES, normalized enrichment scores; PC, principal component; RT-PCR, real time reverse transcription polymerase chain reaction; scRNA-Seq, single cell RNA sequencing; TNF, tumor necrosis factor; UMAP, uniform manifold approximation and projection.

* Corresponding author. Department of Orthopaedic Surgery, UConn Health, Farmington, CT 06030-4037, USA. Tel.: +860 679 7978; fax: +860 679 1474
E-mail addresses: canalis@uchc.edu (E. Canalis), schilling@uchc.edu, denker@uchc.edu (E. Denker).

https://doi.org/10.1016/j.ocarto.2024.100528
Received 30 July 2024; Accepted 4 October 2024

TNFα is a proinflammatory cytokine primarily produced by activated macrophages and known to induce the expression of *Il6* and *Il1b* and promote the release of matrix metalloproteinases resulting in cartilage tissue degradation [10–12]. TNFα inhibits chondrogenesis and this may impair cartilage restoration in conditions of TNFα induced inflammation [13,14]. While these studies document that TNFα plays a role in the pathogenesis of the inflammatory response in cartilage, the cellular composition of cartilage is complex, and the cellular responses to TNFα are heterogeneous [15]. Moreover, recent work in murine models of post-traumatic osteoarthritis revealed transcriptomic heterogeneity in this cellular environment [16]. Therefore, the cells responsible for a given event and its impact on chondrogenesis and inflammation need to be defined at a single cell (sc) resolution. The effect of TNFα on the transcriptomic profile of cartilage at this level of resolution is unknown and should provide clues about the mechanisms responsible for its effects in the joint and its role in inflammation and chondrogenic repair.

To understand the mechanisms involved in the TNFα-dependent inflammatory response in the chondrocyte environment, we explored the transcriptome profile affected by TNFα at a global and sc resolution in murine epiphyseal chondroblasts. To this end, transcriptomes of epiphyseal chondrocytes with chondroblast-like properties were obtained from newborn C57BL/6 mice treated with TNFα and examined using bulk, as well as sc RNA-Sequencing (Seq) approaches.

2. Methods

2.1. Chondrocyte cultures

Cells were isolated from the epiphyses of long bones of the hind limbs from 3- to 4-day-old C57BL/6 mice. Following the dissection of surrounding tissues under a Unitron Z850 stereo microscope, the epiphyseal cartilage was obtained from the proximal and distal joints of the tibiae from 4 mice and placed in high glucose Dulbecco's modified Eagle's medium (DMEM, Life Technologies, Grand Island, NY), as described [17]. The epiphyseal cartilage was exposed to 0.25 % trypsin, 0.9 mM EDTA (Life Technologies), and subsequently with 200 U/ml of type II collagenase (Worthington Biochemical Corporation, Lakewood, NJ) at 37 °C. Following digestion, the tissue was strained through a 70 μm membrane and cells collected by centrifugation and cultured in DMEM supplemented with 10 % heat inactivated fetal bovine serum (FBS, Atlanta Biologics, Atlanta, GA) at a temperature of 37 °C in a humidified 5 % CO_2 atmosphere until reaching ~70 %–80 % confluence [17,18]. Cultures were trypsinized once and cells were seeded at a density of 1 million cells/39.3 cm^2 and cultured to ~70–80 % confluency for 24 h prior to being transferred to DMEM in the absence of serum for 2 h and then exposed to TNFα (Peprotech, Thermo Fisher Scientific, Cranbury, NJ) 50 ng/ml (suspended in phosphate buffered saline and diluted 1:300 in culture medium) for 6 h, for experiments geared to RNA determinations and bulk RNA-Seq, and for 18 h for scRNA-Seq. The higher concentration of TNFα was based on prior work from our laboratory and was chosen to ensure a biological response [8]. The 18 h treatment with TNFα for scRNA-Seq was necessary to allow sufficient time to process the samples for scRNA-Seq immediately at the conclusion of the culture period; the microfluidic partitioning to capture, barcode and process scs was conducted over 6–8 h without interruptions. Preliminary experiments did not reveal substantial differences in the response of chondrocytes to TNFα between 6 h and 18 h of exposure (data not shown). Cells were seeded as a pool for RNA and bulk RNA-Seq experiments and maintained as biological replicates (n = 4) for scRNA-Seq and then pooled immediately prior to microfluidic partitioning. Animal studies were limited to euthanasia of newborn mice for the purpose of tissue harvest and were approved by the Institutional Animal Care and Use Committee of UConn Health, protocol AP-200630-0325.

2.2. Real time reverse transcription polymerase chain reaction (RT-PCR)

Total RNA was extracted using the RNeasy Mini kit (Qiagen, Valencia, CA). Equal amounts of RNA were reverse-transcribed using the iScript RT-PCR kit (BioRad, Hercules, CA) prior to amplification in the presence of specific primers (all from Integrated DNA Technologies, IDT) with the SsoAdvanced™ Universal SYBR Green Supermix (BioRad) at 60°C for 40

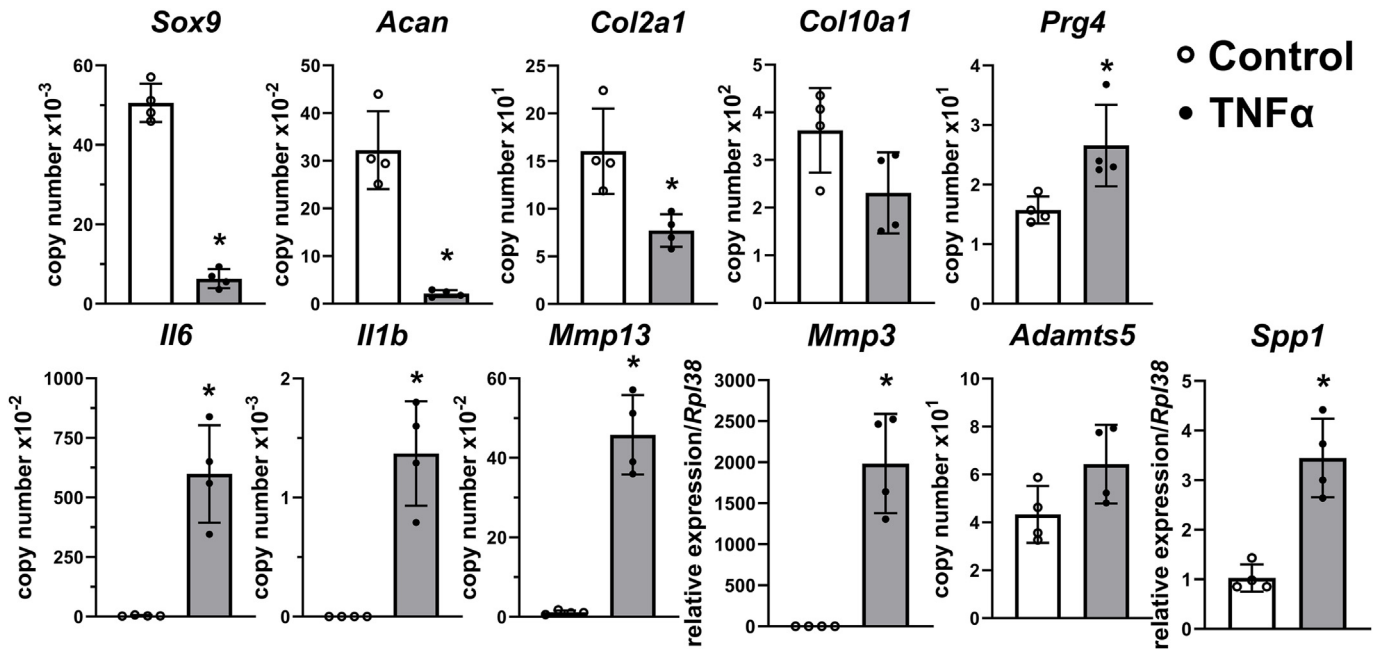

Fig. 1. TNFα inhibits gene markers of chondrocyte differentiation and induces cytokines associated with inflammation and osteoarthritis. Epiphyseal chondrocytes from newborn mice were cultured to ~70 % confluence and treated with TNFα 50 ng/ml or vehicle for 6 h. Total RNA was extracted, and gene expression determined by qRT-PCR. Data are expressed as *Sox9*, *Acan*, *Col2a1*, *Col10a1*, *Prg4*, *Il6*, *Il1b*, *Mmp13*, and *Adamts5* copy number corrected for *Rpl38*. *Mmp3* and *Spp1* are expressed as relative values corrected for *Rpl38*. Values are means ± SD and individual values of n = 4 technical replicates in control (white bars, open circles) cultures or cultures treated with TNFα (grey bars, closed circles). *Significantly different between TNFα and control, $p < 0.05$ by unpaired *t*-test.

cycles (Table S1). Copy number was estimated by comparing amplification curves with those of serial dilutions of cDNA for *Acan*, *Adamts5*, *Il1b*, *Il6*, *Col10a1*, *Mmp13*, *Sox9* (Thermo Fisher Scientific, Waltham, MA), *Prg4* (Bioscience, Nottingham, UK), and *Col2a1* (American Type Culture Collection, ATCC, Manassas, VA). Amplification reactions were conducted in CFX96 qRT-PCR detection systems (BioRad), and fluorescence was monitored at the end of the elongation step during every PCR cycle. Data are expressed as copy number except for *Mmp3*, *Spp1*, *Igf1*, *Igf2*, *Igfbp1*, *2*, *3*, *4*, *5* and *6*, which are expressed as relative to control mRNA normalized to 1. All transcript data were corrected for *Rpl38* expression estimated by comparison to a serial dilution of cDNA for *Rpl38* (ATCC).

2.3. Library preparation, bulk RNA sequencing and Bioinformatics analysis

Total RNA was quantified, and a NanoDrop 2000 spectrophotometer (Thermo Fisher Scientific) was used to determine purity ratios prior to quality analysis which was performed on an Agilent TapeStation 4200 (Agilent Technologies, Santa Clara, CA) using the RNA High Sensitivity assay. Samples used for library preparation had an RNA Integrity Number ≥9.0 and were processed for mRNA-sequencing at the UConn Center for Genome Innovation using the Illumina TruSeq Stranded mRNA sample preparation kit following manufacturer's instructions (Illumina, San Diego, CA), as described previously [8]. Libraries were validated for length and adapter dimer removal using the Agilent TapeStation 4200 D1000 High Sensitivity assay (Agilent Technologies), quantified and normalized using the dsDNA High Sensitivity Assay for Qubit 3.0 (Thermo Fisher Scientific), as previously reported [8]. Sample libraries were prepared for sequencing by denaturing and diluting the libraries per manufacturer's protocol (Illumina). Samples were pooled for sequencing, normalized and run across an Illumina Next-Seq 500 using version 2.5 chemistry. Target read depth was achieved for each sample with paired end 75 bp reads. Following sequencing, raw reads were trimmed with Sickle (Version 1.33), with a quality and length threshold of 30 and 45,

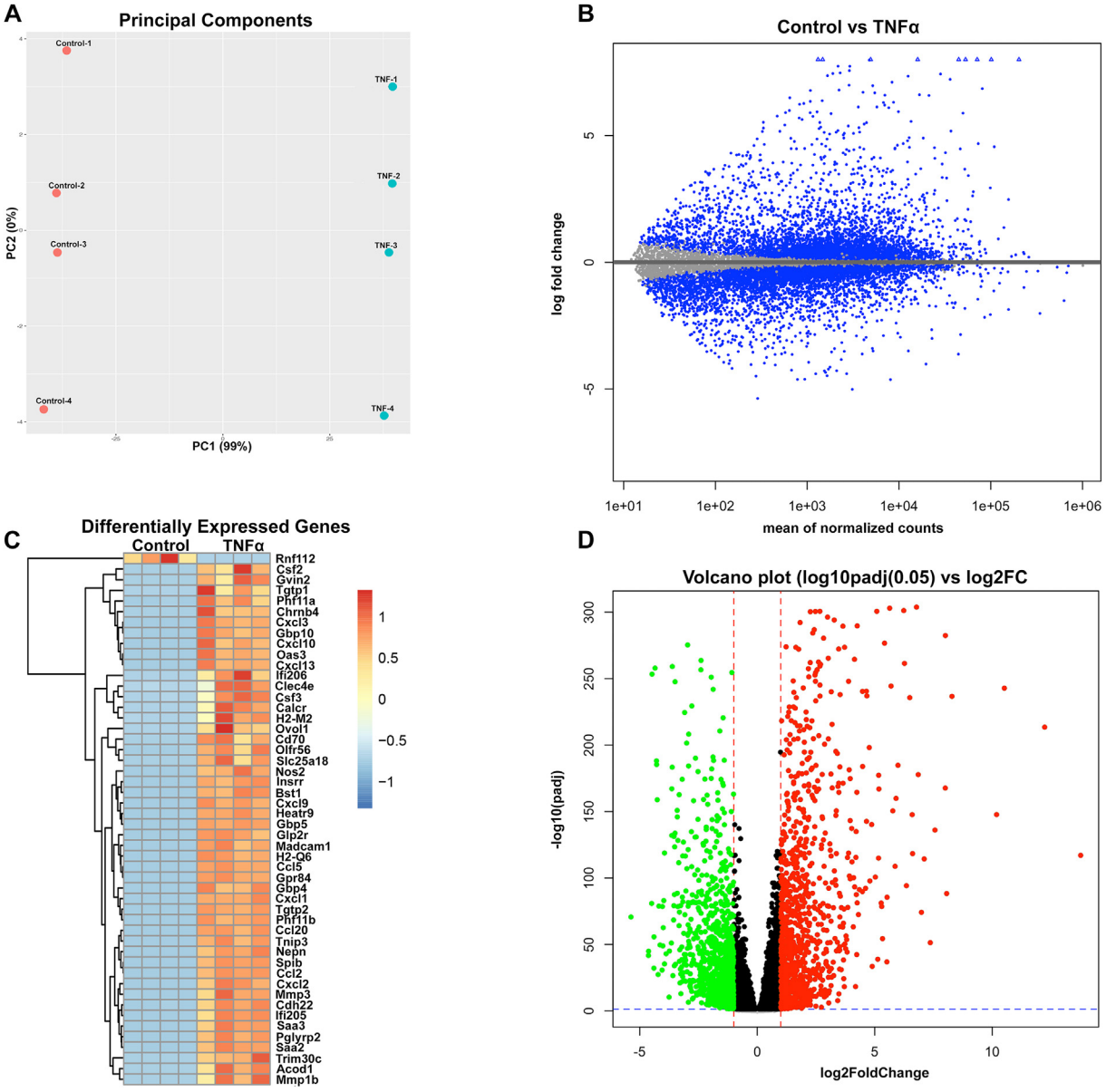

Fig. 2. RNA-Seq transcriptional profile of TNFα-treated chondrocytes. Epiphyseal chondrocytes were cultured to ~70 % confluence and treated with TNFα at 50 ng/ml or vehicle for 6 h. Cells were collected for total RNA and analyzed by RNA-Seq. A. PC analysis of RNA-Seq technical replicates (n = 4 for TNFα and for control). B. Differentially expressed genes as log fold change over means of normalized counts. C. Heat map of the 50 most differentially regulated genes between TNFα and vehicle treated chondrocytes and D. Corresponding volcano plots log2 fold change FDR *p* adjusted value 0.05 for C. and D.

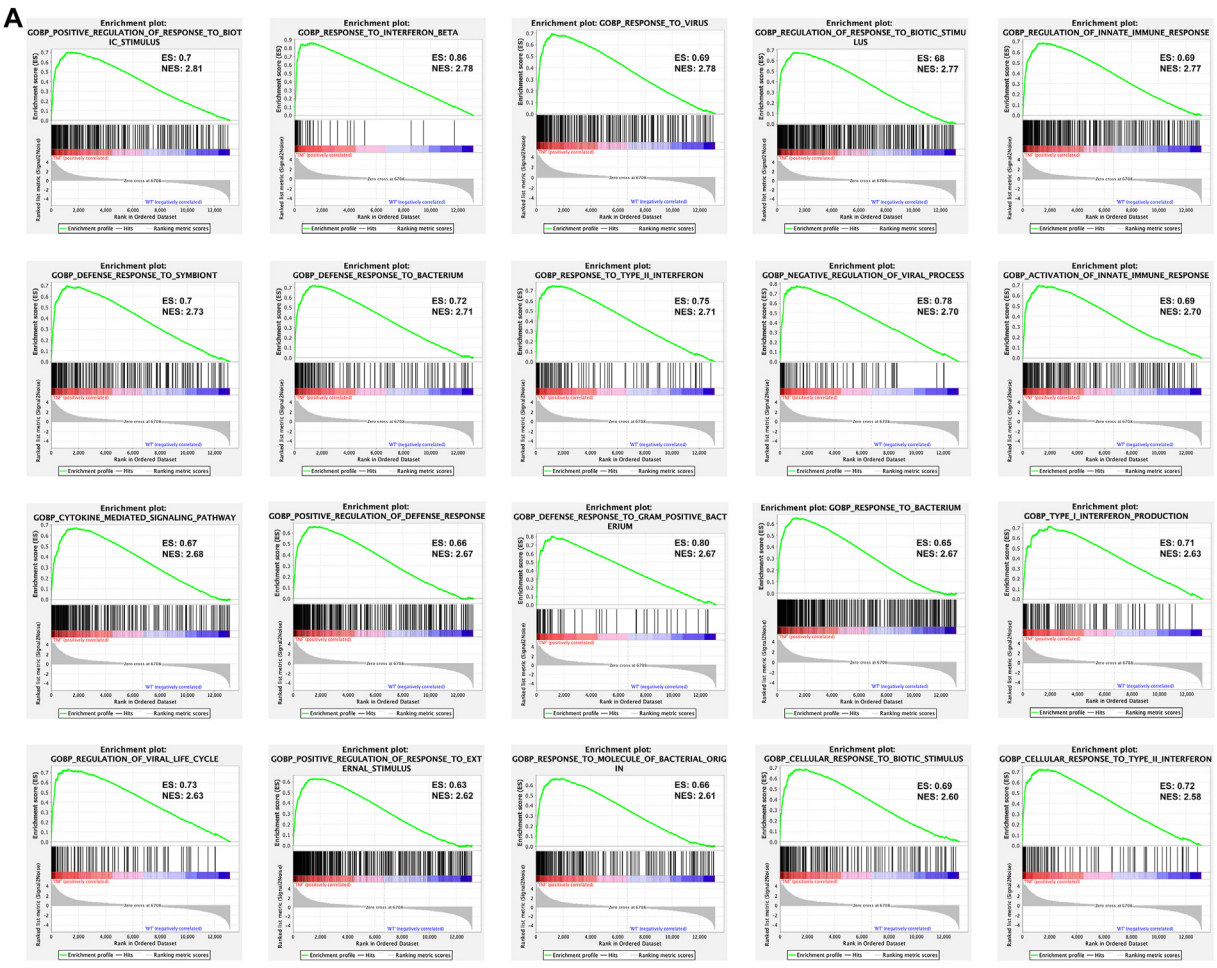

Fig. 3. TNFα enhances the immune and defense response and suppresses cartilage and skeletal development. A. GSEA of biological pathways in epiphyseal chondrocytes treated with TNFα at 50 ng/ml or vehicle for 6 h (n = 4 technical replicates for both). Enrichment scores (ES) and normalized ES of pathways affected by TNFα at a FDR of <0.05 are shown. B. Visualization of gene enrichment analysis, shown as a lollipop chart. Gene count and pathways affected at a *p* adjusted <0.05 are shown.

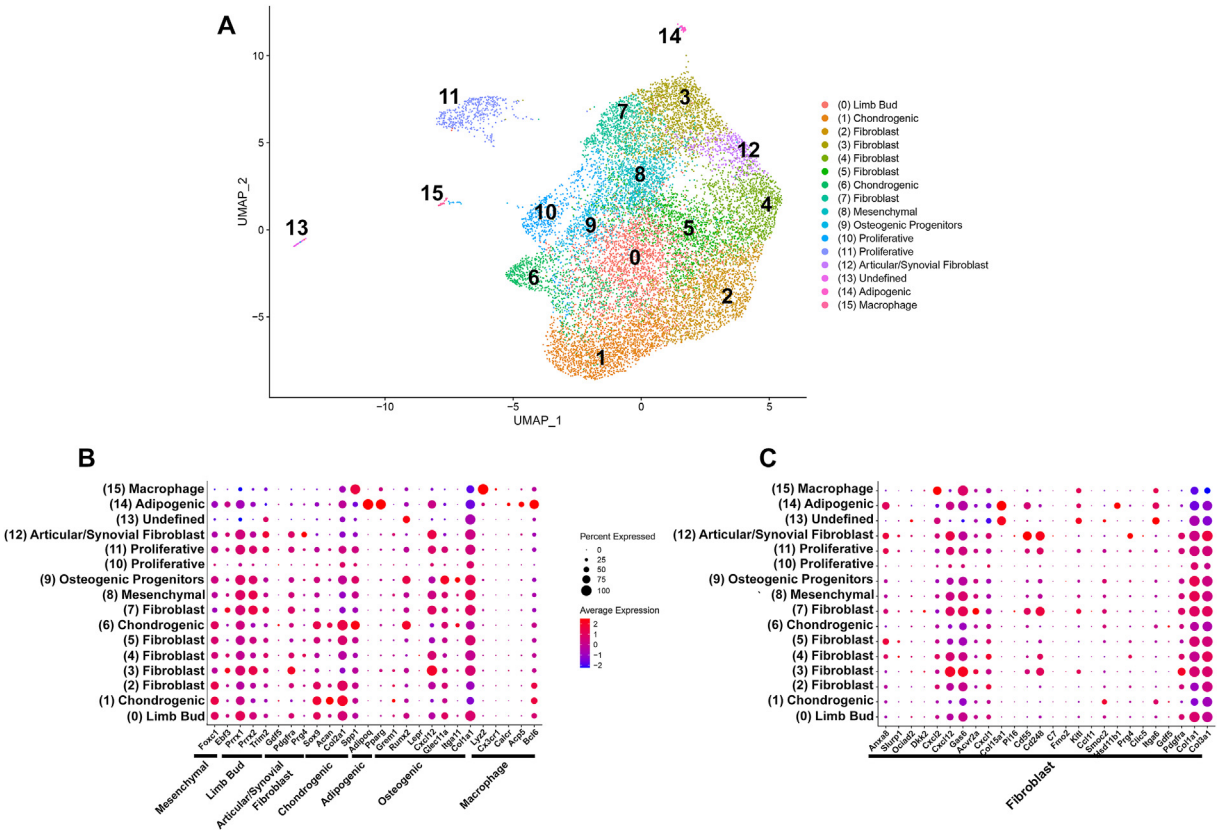

Fig. 4. Uniform manifold approximation and projection (UMAP) for dimension reduction of scRNA-Seq data of epiphyseal chondrocytes from newborn mice reveals 16 cell clusters. A. UMAP visualization of 16 cell clusters of normalized pooled data from epiphyseal chondrocytes from newborn mice cultured to ~70 % confluence and treated with TNFα 50 ng/ml or vehicle for 18 h. B. Dot plot displaying the expression of genes associated with mesenchymal cells, limb bud, articular/synovial cells, chondrogenic, adipogenic and osteogenic cells and macrophages among 16 cellular clusters from epiphyseal chondrocytes from newborn mice identified by UMAP. C. Dot plot displaying the expression of genes associated with fibroblasts in 16 cellular clusters from epiphyseal chondrocytes from newborn mice identified by UMAP. Red denotes higher and blue denotes lower than average expression, and the size of the circle represents the percentage of cells expressing each gene.

respectively, and mapped to the *Mus musculus* genome (GRCm39 ensembl release 105) with HISAT2 (version 2.1.0) [19]. SAM files were obtained and transformed into a BAM format using samtools (version 1.9), and PICARD was used for the removal of PCR duplicates [20]. The counts were generated against the features with HTSeq-count, and the differential gene expression between control and TNFα treated cultures was determined using DESeq2 [21,22]. Covariates were introduced in the DESeq2 analysis to increase accuracy of the results, and genes showing less than ten counts across the compared samples were excluded from further analysis. A false discovery rate adjusted p value < 0.05 was considered significant and used in downstream analysis, as indicated in text and legends. Highly variable functions were identified, and linear dimensional reduction conducted by Principal component (PC) analysis. The processed RNA-Seq results were analyzed by gene set enrichment analysis (GSEA) and using the R package clusterProfiler enrichment tool [23,24].

2.4. ScRNA sequencing and Computational analysis

Transcriptomes from epiphyseal chondroblasts were analyzed on a cell-by-cell basis through the use of microfluidic partitioning to capture scs. Cells from control and TNFα treated cultures were pooled at the completion of the culture and counted on a Cellometer K2 (Nexceleron, Lawrence, MA). Ten thousand live control and experimental cells, respectively, were processed on a Chromium iX instrument using a Chromium sc 3′ library and Gel Bead Kit V3.1 (10x Genomics, Pleasanton, CA) to prepare barcoded libraries, as previously reported [25]. The sc gene expression kit used has a cell capture efficiency of ~65 % and is capable of recovering 500–10,000 cells/lane. Following reverse transcription, libraries were sequenced at the UConn Center for Genome Innovation. cDNAs from a sc had a unique barcode, allowing the sequencing reads to be mapped backed to the cell of origin [26].

FASTQ files were generated using reference genome mm10-2020-A and analyzed using Cell Ranger v7.0 (10x Genomics) for sample demultiplexing, barcode processing and counting of transcripts and output HTMLs for data quality assessment and sample visualization. Secondary analyses of output files were conducted using the Seurat R Package (v4.4) and it included dimensionality reduction, cell clustering and differential gene expression [27,28]. Cells expressing <250 transcripts, >10 % mitochondrial RNA or >10,000 genes/cell were excluded manually, and the data set was normalized by employing the NormalizeData function in Seurat. Highly variable functions were identified, and linear dimensional reduction conducted by PC analysis and non-linear dimension reduction performed by uniform manifold approximation and projection (UMAP) for nonlinear dimensional reduction. Doublets were identified and excluded, and cell clusters were classified according to their gene profile and gene ontology. Pseudotime trajectory analysis of pooled and independent data from epiphyseal chondrocytes treated with TNFα, or vehicle was constructed by analysis of the Seurat object in Monocle 3 [29]. Monocle 3 cell data set was constructed and the learn principal graph from the reduced dimensional space was applied using learn_graph, as previously described [25]. Cells were organized along their trajectory using Monocle plot_cells and order_cells; marker genes for each cluster were identified using the Seurat's FindAllMarkers function.

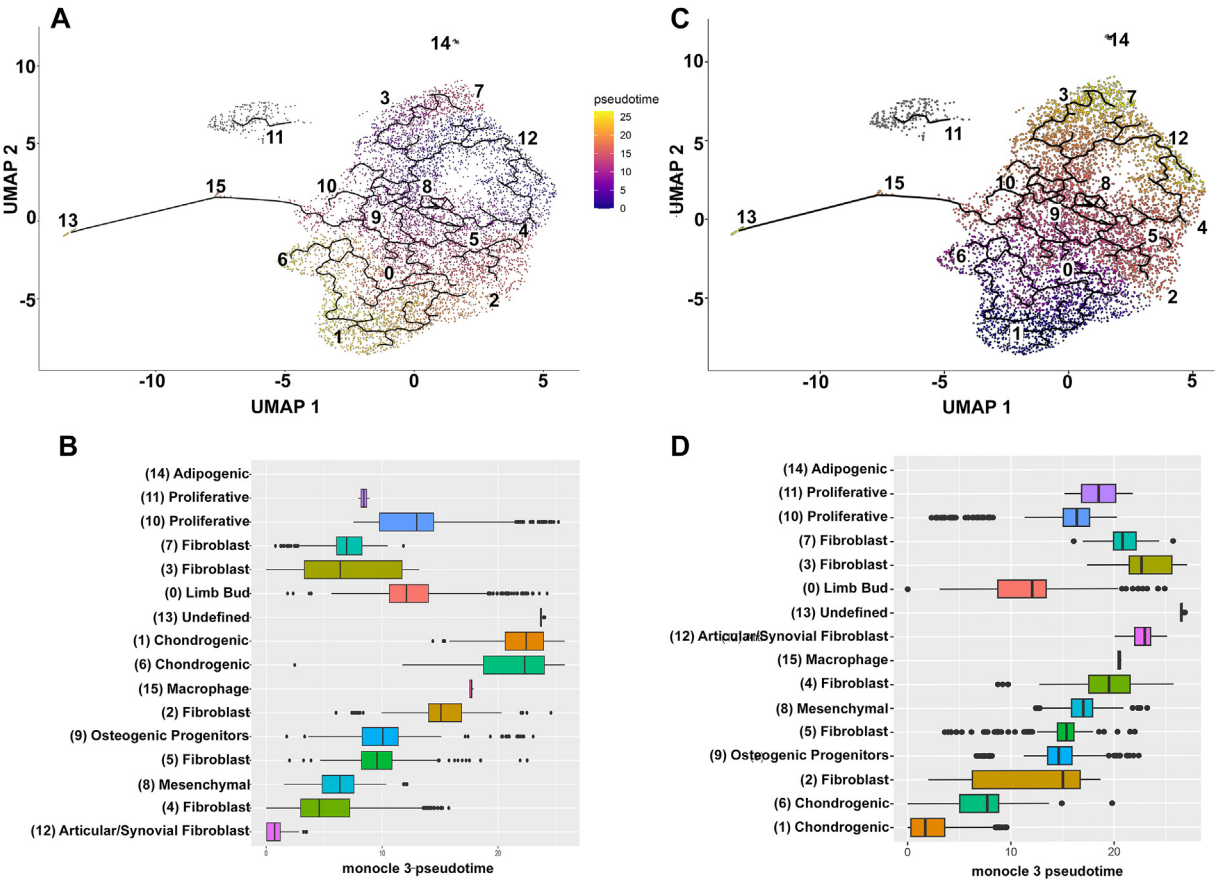

Fig. 5. Trajectory and pseudotime analysis define cell differentiation pathways among cell clusters identified in epiphyseal chondrocytes from newborn mice. Trajectory and pseudotime analysis was performed using Monocle 3 in pooled data from epiphyseal chondrocytes cultured to ~70 % confluence and treated with TNFα 50 ng/ml or vehicle for 18 h. Pseudotime analysis of 16 cellular clusters identified in epiphyseal chondrocytes by UMAP shown in Fig. 4. In A. and B. articular/synovial fibroblast cluster was used as a root node and in C. and D. the chondrogenic cluster was used as a root node. An alternative visualization or the pseudotime UMAP as a progression boxplot of pseudotime values is shown in B. and D.

Gene ontology and Ingenuity Pathway Analysis (IPA, Qiagen, Redwood City, CA) of differentially expressed genes was performed on a per-cluster basis, and genes prioritized based on ontology, and relevance to transcriptional control and signaling pathways [23,24,30]. IPA was performed to analyze canonical pathways under the Genes and Chemicals category.

2.5. Statistics

RT-PCR data are expressed as means ± S.D. and individual values. Statistical differences were determined by unpaired Student's t-test.

3. Results

3.1. TNFα suppresses gene markers of chondrocyte differentiation and enhances inflammation in epiphyseal chondrocytes

To determine the role of TNFα in chondrogenesis and inflammation in cartilage, epiphyseal chondrocytes were cultured and treated with TNFα or vehicle under serum free conditions. TNFα at 50 ng/ml for 6 h decreased the expression of chondrogenic gene markers, including *Sox9*, *Acan* and *Col2a1*, as well as *Col10a1*, but not *Prg4* (Fig. 1). TNFα enhanced the expression of *Il6* and *Il1b*, *Mmp3*, *Mmp13* (all $p < 0.05$) and *Adamts5* (NS), encoding pro-inflammatory cytokines and proteases, in epiphyseal chondrocytes (Fig. 1). In addition, TNFα induced *Spp1*, encoding secreted phosphoprotein 1. The results confirm that TNFα inhibits chondrogenesis and enhances the inflammatory response and the potential for matrix degradation in epiphyseal chondrocytes [8,13].

To understand potential molecular mechanisms associated with the effect of TNFα on murine epiphyseal cartilage, RNA from TNFα-treated and control epiphyseal chondrocytes was examined by bulk RNA-Seq analysis. PC analysis revealed segregation between control and experimental samples and there were 2738 ≥ log2FC1 and *p* adjusted <0.05 differentially regulated genes between TNFα and control chondrocytes; 1380 genes were upregulated and 1358 were downregulated by TNFα (Fig. 2). GSEA of biological pathways revealed enrichment of genes associated with enhanced response to biotic stimulus, the immune and defense response, cytokine mediated signaling and cellular response to interferon B in TNFα-treated cells compared to control cells (Fig. 3A). Further functional gene enrichment analysis of the biological pathways affected, using the R package clusterProfiler, confirmed activation of these pathways and suppression of cartilage and connective tissue development, skeletal morphogenesis and development, and canonical Wnt signaling in TNFα-treated chondrocytes compared to control cells (Fig. 3B). In accordance, the gene targets of Wnt signaling *Axin2* and *Ccn4* were downregulated by TNFα (log2FC) 0.2 and 0.6, respectively, and the Wnt antagonist *Dkk1*, induced 6.2 although its levels of expression were low [31].

3.2. ScRNA-Sequencing reveals unique cell clusters in epiphyseal chondrocytes

scRNA-Seq was conducted on epiphyseal chondrocytes from newborn C57BL/6 mice cultured to ~70 % confluence, by processing the cells in a Chromium iX using a 3′ library kit (10x Genomics). An equal number of live cells (~10,000 each) from control and TNFα-treated samples were processed on a Chromium iX instrument and an estimated 14,616 cells

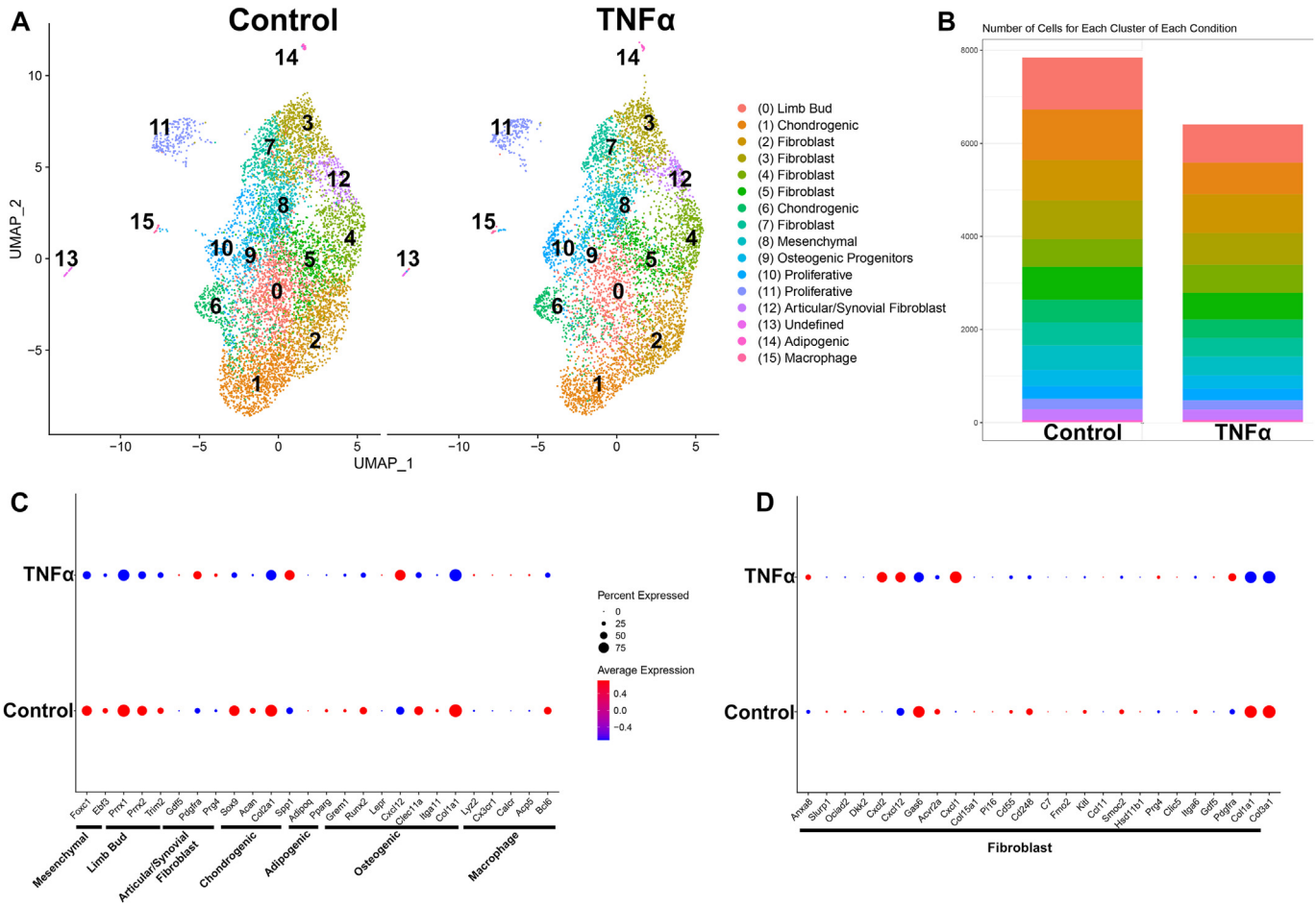

Fig. 6. Uniform manifold approximation and projection (UMAP) for dimension reduction of scRNA-Seq data and differential gene expression in distinct cellular clusters from epiphyseal chondrocytes treated with TNFα. A. UMAP visualization of 16 cell clusters of normalized data from epiphyseal chondrocytes analyzed independently in cells treated with TNFα 50 ng/ml or treated with vehicle (control) for 18 h. B. Bar graph demonstrates the cell distribution present in each individual cluster from chondrocytes treated with either TNFα or vehicle. Dot plot displaying the effect of TNFα compared to control on the expression of genes associated in C. with mesenchymal cells, limb bud articular/synovial, chondrogenic, adipogenic and osteogenic cells and macrophages, and in D. with fibroblast cell clusters present in epiphyseal chondrocytes treated with TNFα 50 ng/ml or vehicle (control) for 18 h. Red denotes higher and blue denotes lower than average expression, and the size of the circle represents the percentage of cells expressing each gene. Data were scaled so that they were standardized to have a mean of 0 and a standard deviation of 1.

were recovered. Following normalization cells with >10 % mitochondrial RNA, <250 transcripts and >10,000 genes/cell were excluded. Normalization and doublet filtering and exclusion reduced the number of cells analyzed to 14,239, with 24,320 unique genes analyzed. Clustering analysis of epiphyseal chondrocytes (pooled data from cells treated with TNFα or vehicle) using the UMAP for non-linear dimensional reduction algorithm, accurately distinguished 16 different cell clusters, although 3 of the clusters (undefined, adipogenic and macrophages) represented <1 % of the cell population (Fig. 4A, Table S2) [32]. The more prevalent clusters were constituted by cells with a transcriptome profile of limb bud (cluster 0), chondrogenic (clusters 1 and 6) and fibroblasts (clusters 2, 3, 4, 5 and 7) and these constituted ~73 % of the cell population analyzed (Table S2).

Cells from the chondrogenic clusters expressed genes known to be associated with chondrocytes, including *Sox9*, *Acan* and *Col2a1* and the articular/synovial cluster expressed *Prg4* and *Pdgfra* (Fig. 4B–Table S3) [33]. Genes known to be expressed by joint fibroblasts were detected in 5 clusters that comprised ~45 % of the cells isolated from epiphyseal chondrocytes (Fig. 4C). Pseudotime trajectory finding was constructed with Monocle 3 and used to predict the differentiation trajectory among clusters present in epiphyseal chondrocytes. Pseudotime trajectory finding selecting clusters expressing articular/synovial fibroblasts or chondrogenic cells as a root node revealed an association between fibroblasts and chondrogenic clusters (Fig. 5).

3.3. *TNFα influences gene expression and cluster distribution in epiphyseal chondrocytes*

Independent clustering analysis of epiphyseal chondrocytes treated with TNFα revealed an overall decrease (18.5 %) of cells recovered compared to control cells. The most affected cell clusters by TNFα were the chondrogenic clusters [1and6] that were suppressed by 32 % and the limb bud cluster (0) that was suppressed by 27 % relative to controls (Fig. 6, Tables S2 and S4). After correction for the overall (18.5 %) decrease in cells recovered following TNFα treatment, TNFα decreased the chondrogenic and the limb bud clusters by 16 % and 10 %, respectively, and decreased the mesenchymal cell cluster by 7 % whereas other cell clusters were not affected substantially.

Independent analysis of gene expression among the 16 cellular clusters from epiphyseal chondrocytes treated with TNFα revealed decreased expression of genes associated with the limb bud, chondrogenic and osteogenic cluster, except for *Cxcl12* and *Spp1* that were detected in a greater number of cells from cultures exposed to TNFα (Fig. 6C–Tables S5A, S6A, S6B). TNFα increased the expression of the articular/synovial fibroblast-associated genes *Gdf5*, *Pdgfra* and *Prg4*, although the percent of cells expressing *Gdf5* was small. TNFα decreased the expression of selected genes associated with the fibroblast clusters including *Gas6*, *Acvr2a*, *Col1a1* and *Col3a1* and increased the level of

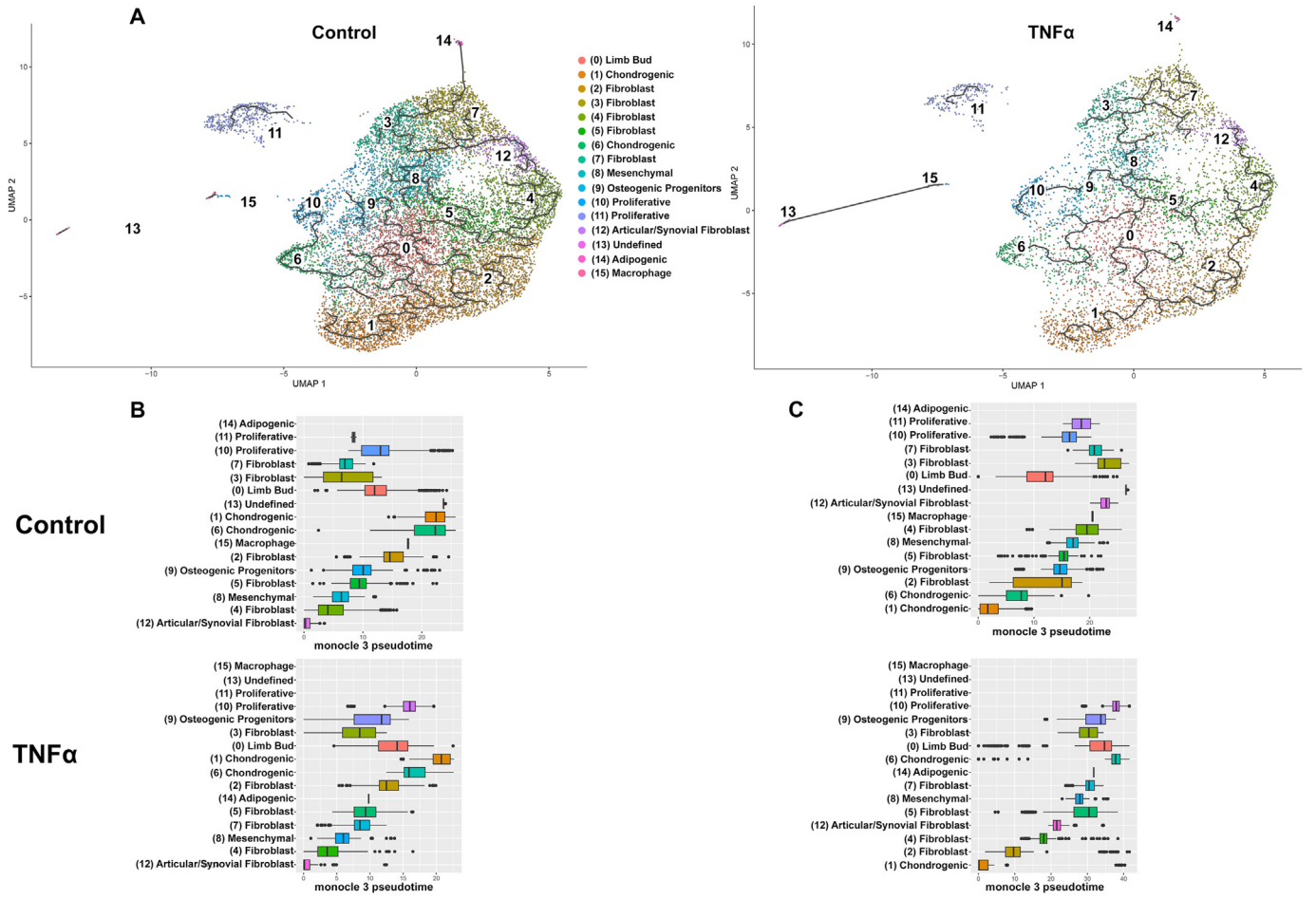

Fig. 7. Trajectory and pseudotime analysis define cell differentiation pathways among cell clusters identified in epiphyseal chondrocytes treated with TNFα. Trajectory analysis was performed using Monocle 3 in independent sc RNA-Seq data from epiphyseal chondrocytes cultured either in the presence of TNFα 50 ng/ml or vehicle (control) for 18 h. A. Trajectory analysis of the 16 cellular clusters identified by UMAP in Fig. 6. B. and C. Pseudotime analysis of UMAP as a progression boxplot of pseudotime values using either the articular/synovial cell cluster as a root node in B. or the chondrogenic cluster as a root node in C.

expression of *Cxcl1*, *Cxcl2*, *Cxcl12* and *Pdgfra* (Fig. 6D–Table S5B and S6A). Changes in gene expression were verified by bulk RNA-Seq (Figure S1). Pseudotime trajectory analysis demonstrated modest changes between control and TNFα treated epiphyseal chondrocytes, whether the articular/synovial fibroblast or the chondrogenic cluster was used as a root node (Fig. 7).

IPA of canonical pathways was conducted in pooled chondrogenic (clusters 1 and 6), pooled fibroblast (clusters 2, 3, 4, 5 and 7), mesenchymal cells, osteogenic and proliferative cells (clusters 10 and 11) and articular/synovial cells (cluster 12) (Figure S2). Clusters expressing <100 genes were excluded. Compared to control cultures, IPA revealed enhancement of the osteoarthritis pathway by TNFα in chondrogenic clusters, enhanced rheumatoid arthritis and pathogen induced cytokine storm signaling pathway in fibroblast clusters and IL-6 and IL-33 signaling in the mesenchymal cluster. IL-17 signaling was induced only in mesenchymal and fibroblast clusters of control cultures, whereas fibroblast growth factor signaling was induced only in the fibroblast control clusters suggesting suppression of these signals by TNFα.

3.4. TNFα regulates the IGF-IGF binding protein axis in epiphyseal chondrocytes

To explore for possible explanations of the inhibitory action of TNFα on genes associated with cartilage and skeletal development, as determined by GSEA (Fig. 3), we determined its effect on the insulin-like growth factor (IGF)-IGF binding protein (IGFBP) axis. TNFα suppressed *Igf1* and *Igf2* expression as determined by bulk RNA-Seq and RT-PCR of epiphyseal chondrocytes (Fig. 8, Table S5C). TNFα induced the inhibitory IGFBPs *Igfbp3* and *Igfbp5*, suppressed *Igfbp4* and had a small non-significant inhibitory effect on *Igfpb2* and *Igfpb6*. *Igfbp1* was not detected. *Igf1* was mostly expressed by macrophages and *Igf2* by the chondrogenic cluster and *Igfbp2*, *3*, *4*, *5* and *6* were detected in all clusters with a somewhat more prevalent expression by fibroblast clusters.

4. Discussion

In previous work, we demonstrated that the inflammatory response to TNFα in epiphyseal chondrocytes is enhanced in the context of a gain-of-NOTCH2 function and together they induce pathways associated with osteoarthritis and the phagosome [8]. The present study extends those observations and explores in detail the effects of TNFα and mechanisms responsible for an inflammatory response by analyzing transcriptome profiles of epiphyseal chondrocytes treated with TNFα at a bulk and sc resolution. Confirming prior observations, we demonstrate that TNFα suppresses selected gene markers of differentiated chondrocytes and induces proinflammatory cytokines and MMPs [8,13]. GSEA of bulk RNA-Seq data from epiphyseal chondrocytes revealed that TNFα enhances the response to biotic stimulus, the defense and immune response and cytokine mediated signaling and suppresses cartilage and skeletal morphogenesis and development. RNA-Seq and qRT-PCR of RNA extracts demonstrated upregulation of *Il1b*, *Il6* and *Mmp13* by TNFα, and a marked induction of *Mmp3*, encoding the matrix protease stromelysin.

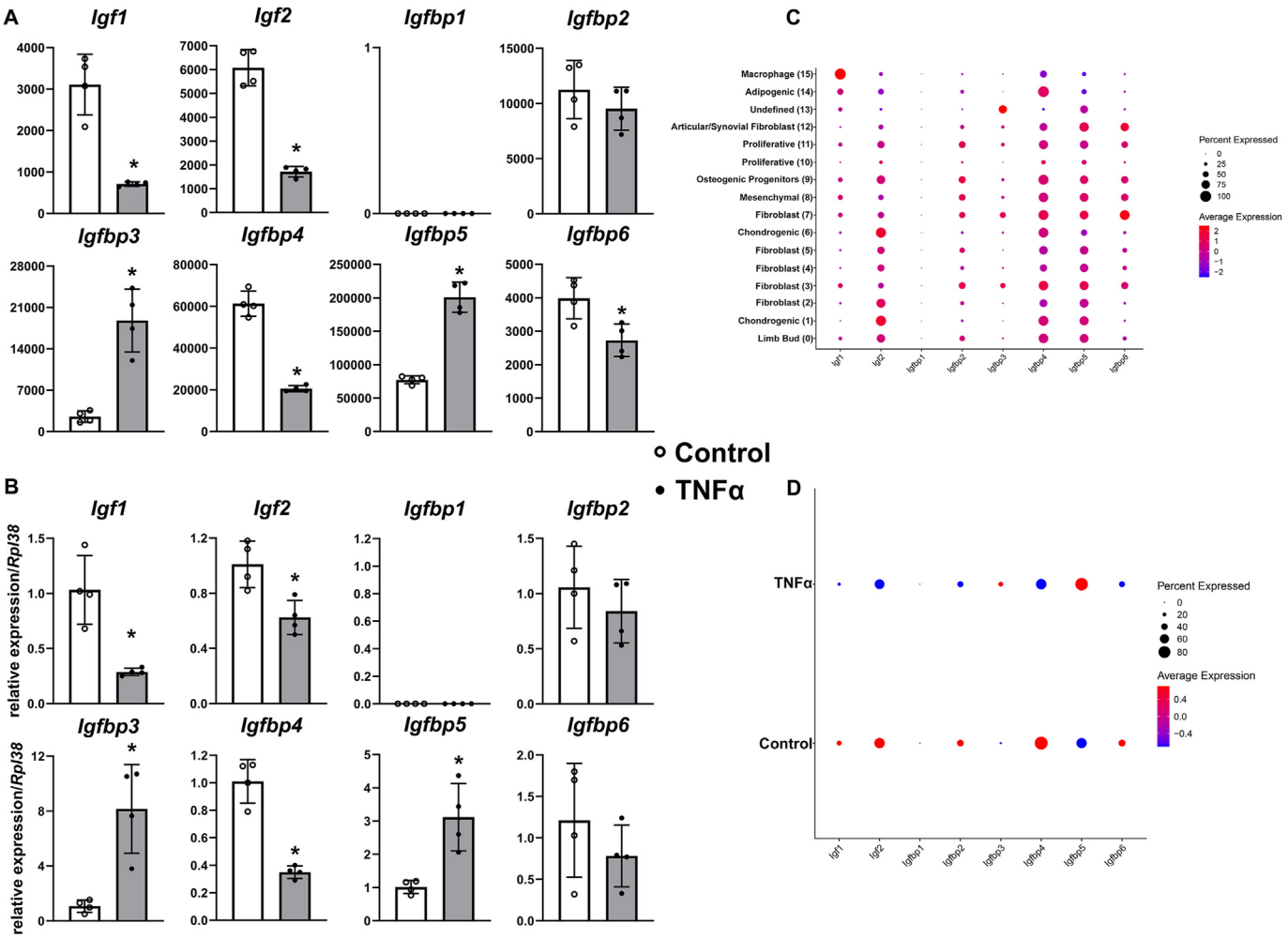

Fig. 8. TNFα inhibits *Igf1* and *Igf2* and regulates *Igfbp* transcripts in epiphyseal chondrocytes. RT-PCR, bulk and sc RNA-Seq analysis of epiphyseal chondrocytes cultured to ~70 % confluence and treated with TNFα 50 ng/ml or vehicle for 6 h for RT-PCR and bulk RNA-Seq, and for 18 h for scRNA-Seq. In A. Number of fragments mapping to the gene of interest determined by bulk RNA-Seq, and in B. mRNA expression determined by RT-PCR of *Igf1*, *Igf2* and *Igfbp1*, *2*, *3*, *4*, *5* and *6* both shown as means ± SD and individual values; n = 4 technical replicates in control (white bars, open circles) cultures or cultures treated with TNFα (grey bars, closed circles). *Significantly different between TNFα and control, $p < 0.05$ by unpaired *t*-test. In C. and D. dot plot displaying *Igf1*, *Igf2* and *Igfbp1*, *2*, *3*, *4*, *5* and *6* in C. in 16 cellular clusters identified in epiphyseal chondrocytes, and in D. showing the effect of TNFα. Red denotes higher, and blue denotes lower than average expression, and the size of the circle represents the percentage of cells expressing each gene. Data were scaled so that they were standardized to have a mean of 0 and a standard deviation of 1.

The upregulation of these cytokines and MMPs by TNFα could play a role in the inflammatory response and matrix degradation associated with osteoarthritis. Due to its broad substrate specificity and expression by osteoblasts and chondrocytes, stromelysin plays an important role in tissue remodeling [34].

To explore the molecular processes occurring during the inflammatory response to TNFα, we performed scRNA-Seq analysis of confluent epiphyseal chondrocytes with chondroblast-like properties treated with TNFα or vehicle. scRNA-Seq in combination with bulk RNA-Seq were used as complementary approaches to analyze the transcriptome of epiphyseal chondrocytes in the context of TNFα. scRNA-Seq was particularly useful in the analysis of a complex cell culture model allowing us to discern the transcriptome profile of various cell populations present in epiphyseal chondrocytes and to study the TNFα-dependent changes in cell composition and how these modulate chondrogenesis and inflammation.

scRNA-Seq analysis revealed cellular heterogeneity in epiphyseal chondroblast cultures confirming prior observations in epiphyseal, growth plate and articular cartilage [16,35–37]. We identified 16 cell clusters and pseudotime trajectory analysis revealed an association between clusters expressing gene markers identified in chondrogenic cells, articular/synovial fibroblasts and fibroblasts. Although previous work in postnatal femoral and tibial epiphyses revealed the presence of 34 clusters, the characterization of cell clusters present in epiphyseal chondroblasts by UMAP performed in the present study is by and large consistent with previous findings in postnatal epiphyses [35].

scRNA-Seq analysis revealed cellular heterogeneity in epiphyseal chondrocyte cultures and pseudotime trajectory analysis revealed an association between clusters expressing gene markers identified in fibroblasts and chondrogenic cells. This potential progression was not affected by TNFα. It is of interest that cluster analysis identified 5 clusters associated with fibroblasts and these constituted ~40 % of the cell population recovered. It is important to note that the cell population of each cluster defined by its transcriptome profile is related but not necessarily completely homogeneous.

Our study revealed the presence of the same cell clusters in control and TNFα treated epiphyseal chondroblasts. Although an equal number of live cells from control and TNFα-treated cultures were partitioned on a Chromium iX instrument, the overall number of cells recovered was lower in the context of TNFα. There is no apparent explanation for the difference in recovery although it is not likely due to alterations in cell viability or replication since the number of live cells processed was comparable between control and experimental groups. In accordance with the known

inhibitory effects of TNFα on chondrogenesis, the clusters mostly affected were those expressing gene profiles of chondrocytes and the limb bud. In addition, TNFα suppressed the expression of limb bud and chondrogenic gene markers in these clusters. It is of interest that TNFα induced *Spp1*, encoding secreted phosphoprotein 1 or osteopontin, in chondrogenic cells and *Spp1* has been associated with inflammation and osteoarthritis [38,39]. scRNA-Seq has confirmed the increased expression of *Spp1* in osteoarthritis, and even though its distribution is heterogeneous, a unique cluster of chondrocytes characterized by high *Spp1* expression was identified [39]. Moreover, IPA revealed enhanced osteoarthritis pathway by TNFα in chondrogenic clusters. The cell heterogeneity of epiphyseal chondrocytes has important implications on the interpretation of the results obtained with this culture model since a change observed may or may not be due to a direct effect on a chondrogenic population.

GSEA of bulk RNA-Seq data revealed suppression of cartilage and skeletal tissue development by TNFα leading us to determine its influence on the IGF/IGFBP axis. The current findings demonstrate the expression of *Igf1* and *Igf2* by multiple clusters from epiphyseal chondrocytes and their downregulation by TNFα, confirming previous observations in hepatocytes and vascular smooth muscle cells [40,41]. It is of interest that *Igf2* was mostly expressed by chondrogenic clusters, and its level of expression was higher than that of *Igf1*, possibly related to the fact that epiphyseal chondrocytes were isolated from newborn mice. These findings are consistent with the essential role played by IGF2 in cartilage development, perichondrial cell proliferation and differentiation and chondrocyte metabolism [42]. TNFα induced *Igfbp3* and *Igfbp5*, binding proteins that have been associated with an inhibitory function of IGF actions, and suppressed *Igfbp4*, a binding protein that has been associated with both stimulatory and inhibitory activity on the IGF axis possibly by modulating the bioavailability of IGF1 [43,44]. The suppression of *Igf1* by TNFα may contribute to its role in inflammation and osteoarthritis, since IGF1 inhibits cartilage matrix degradation and by promoting cartilage anabolism it favors its repair [45].

The profound effects of TNFα on the IGF/IGFBP axis are in agreement with findings in osteoarthritis and rheumatoid arthritis and preclinical models of the disease. Although there is increased IGF1 in synovial fluid and articular chondrocytes and cartilage from individuals with osteoarthritis and rheumatoid arthritis, there is a concomitant increase in IGFBP3 and IGFBP5 and IGFBP3 colocalizes with extracellular matrix proteins, such as fibronectin [46,47]. The increase in IGFBP3 and IGFBP5 in the joint environment may reduce the availability of IGF1 to articular chondrocytes and temper its anabolic effects. Indeed, inhibition of the interaction between IGF1 and IGFBPs results in an increase in available IGF1 and as a consequence an increase in proteoglycan synthesis with improved osteoarthritis in preclinical models of the disease [48,49]. Although estrogen replacement therapy increases IGFBP3 in articular cartilage of ovariectomized cynomolgus monkeys, this does not alter the collagen or proteoglycan content in the tissue or the beneficial effect of estrogen on osteoarthritis [50].

A limitation of this work is the fact that data were restricted to the determination of gene profiles and changes were not confirmed at the protein level. We recognize that epiphyseal chondrocytes from newborn mice have properties of chondroblasts, are not fully mature and are not entirely representative of events occurring in the joint *in vivo*, and that osteoarthritis is a cartilage disorder of mature joints. However, they offered an initial and practical approach to ascertain the cellular environment possibly responsible for the effect of TNFα.

In conclusion, TNFα inhibits chondrogenesis, enhances the inflammatory response and affects cell cluster allocation in epiphyseal chondrocyte cultures.

Author contributions

Ernesto Canalis: Conception and design, analysis and interpretation of the data, drafting of the article, critical revision of the article for important intellectual content, obtaining of funding, final approval of the article. **Lauren Schilling**: Technical support, final approval of the article. **Emily Denker**: Analysis and interpretation of the data, collection and assembly of data, final approval of the article.

Data availability

All data are available from the corresponding author upon a reasonable request. The raw data for bulk and sc RNA-Seq were deposited in Gene Expression Omnibus – GSE268128 and GSE268131.

Funding

This work was supported by a grant from the National Institute of Arthritis and Musculoskeletal and Skin Diseases (NIAMS) AR078149 (EC). The content is solely the responsibility of the authors and does not necessarily represent the official views of the National Institutes of Health.

Declaration of competing interest

The authors declare no conflicts of interest with the contents of this article.

Acknowledgments

The authors thank Mary Yurczak for secretarial assistance.

Appendix A. Supplementary data

Supplementary data to this article can be found online at https://doi.org/10.1016/j.ocarto.2024.100528.

References

[1] B.J. de Lange-Brokaar, A. Ioan-Facsinay, G.J. van Osch, A.M. Zuurmond, J. Schoones, R.E. Toes, et al., Synovial inflammation, immune cells and their cytokines in osteoarthritis: a review, Osteoarthritis Cartilage 20 (2012) 1484–1499, https://doi.org/10.1016/j.joca.2012.08.027.

[2] P.M. van der Kraan, W.B. van den Berg, Chondrocyte hypertrophy and osteoarthritis: role in initiation and progression of cartilage degeneration? Osteoarthritis Cartilage 20 (2012) 223–232, https://doi.org/10.1016/j.joca.2011.12.003.

[3] M. Kloppenburg, F. Berenbaum, Osteoarthritis year in review 2019: epidemiology and therapy, Osteoarthritis Cartilage 28 (2020) 242–248, https://doi.org/10.1016/j.joca.2020.01.002.

[4] M. Kapoor, J. Martel-Pelletier, D. Lajeunesse, J.P. Pelletier, H. Fahmi, Role of proinflammatory cytokines in the pathophysiology of osteoarthritis, Nat. Rev. Rheumatol. 7 (2011) 33–42, https://doi.org/10.1038/nrrheum.2010.196.

[5] R.F. Loeser, S.R. Goldring, C.R. Scanzello, M.B. Goldring, Osteoarthritis: a disease of the joint as an organ, Arthritis Rheum. 64 (2012) 1697–1707, https://doi.org/10.1002/art.34453.

[6] M.B. Goldring, M. Otero, Inflammation in osteoarthritis, Curr. Opin. Rheumatol. 23 (2011) 471–478, https://doi.org/10.1097/BOR.0b013e328349c2b1.

[7] S. Glyn-Jones, A.J. Palmer, R. Agricola, A.J. Price, T.L. Vincent, H. Weinans, et al., Osteoarthritis, Lancet 386 (2015) 376–387, https://doi.org/10.1016/S0140-6736(14)60802-3.

[8] E. Canalis, J. Yu, V. Singh, M. Mocarska, L. Schilling, NOTCH2 sensitizes the chondrocyte to the inflammatory response of tumor necrosis factor α, J. Biol. Chem. 299 (2023) 105372 https://doi.org/10.1016/j.jbc.2023.105372.

[9] J. Yu, E. Canalis, The Hajdu Cheney mutation sensitizes mice to the osteolytic actions of tumor necrosis factor alpha, J. Biol. Chem. 294 (2019) 14203–14214, https://doi.org/10.1074/jbc.RA119.009824.

[10] A.I. Catrina, J. Lampa, S. Ernestam, E af Klint, J. Bratt, L. Klareskog, et al., Anti-tumour necrosis factor (TNF)-alpha therapy (etanercept) down-regulates serum matrix metalloproteinase (MMP)-3 and MMP-1 in rheumatoid arthritis, Rheumatology 41 (2002) 484–489, https://doi.org/10.1093/rheumatology/41.5.484.

[11] Q. Gu, H. Yang, Q. Shi, Macrophages and bone inflammation, J Orthop Translat 10 (2017) 86–93, https://doi.org/10.1016/j.jot.2017.05.002.

[12] S. Kwan Tat, M. Padrines, S. Theoleyre, D. Heymann, Y. Fortun, IL-6, RANKL, TNF-alpha/IL-1: interrelations in bone resorption pathophysiology, Cytokine Growth Factor Rev. 15 (2004) 49–60.

[13] N. Wehling, G.D. Palmer, C. Pilapil, F. Liu, J.W. Wells, P.E. Muller, et al., Interleukin-1beta and tumor necrosis factor alpha inhibit chondrogenesis by human mesenchymal stem cells through NF-kappaB-dependent pathways, Arthritis Rheum. 60 (2009) 801–812, https://doi.org/10.1002/art.24352.

[14] E. Chisari, K.M. Yaghmour, W.S. Khan, The effects of TNF-alpha inhibition on cartilage: a systematic review of preclinical studies, Osteoarthritis Cartilage 28 (2020) 708–718, https://doi.org/10.1016/j.joca.2019.09.008.
[15] M.K. Preedy, M.R.H. White, V. Tergaonkar, Cellular heterogeneity in TNF/TNFR1 signalling: live cell imaging of cell fate decisions in single cells, Cell Death Dis. 15 (2024) 202, https://doi.org/10.1038/s41419-024-06559-z.
[16] A. Sebastian, J.L. McCool, N.R. Hum, D.K. Murugesh, S.P. Wilson, B.A. Christiansen, et al., Single-cell RNA-seq reveals transcriptomic heterogeneity and post-traumatic osteoarthritis-associated early molecular changes in mouse articular chondrocytes, Cells 10 (2021) 1462, https://doi.org/10.3390/cells10061462.
[17] S. Zanotti, E. Canalis, Interleukin 6 mediates select effects of Notch in chondrocytes, Osteoarthritis Cartilage 21 (2013) 1766–1773, https://doi.org/10.1016/j.joca.2013.08.010.
[18] S. Zanotti, E. Canalis, Notch suppresses nuclear factor of activated T cells (NFAT) transactivation and Nfatc1 expression in chondrocytes, Endocrinology 154 (2013) 762–772, https://doi.org/10.1210/en.2012-1925.
[19] D. Kim, B. Langmead, S.L. Salzberg, HISAT: a fast spliced aligner with low memory requirements, Nat. Methods 12 (2015) 357–360, https://doi.org/10.1038/nmeth.3317.
[20] H. Li, B. Handsaker, A. Wysoker, T. Fennell, J. Ruan, N. Homer, et al., The sequence alignment/map format and SAMtools, Bioinformatics 25 (2009) 2078–2079, https://doi.org/10.1093/bioinformatics/btp352.
[21] S. Anders, P.T. Pyl, W. Huber, HTSeq–a Python framework to work with high-throughput sequencing data, Bioinformatics 31 (2015) 166–169, https://doi.org/10.1093/bioinformatics/btu638.
[22] M.I. Love, W. Huber, S. Anders, Moderated estimation of fold change and dispersion for RNA-seq data with DESeq2, Genome Biol. 15 (2014) 550, https://doi.org/10.1186/s13059-014-0550-8.
[23] A. Subramanian, P. Tamayo, V.K. Mootha, S. Mukherjee, B.L. Ebert, M.A. Gillette, et al., Gene set enrichment analysis: a knowledge-based approach for interpreting genome-wide expression profiles, Proc. Natl. Acad. Sci. U. S. A. 102 (2005) 15545–15550, https://doi.org/10.1073/pnas.0506580102.
[24] T. Wu, E. Hu, S. Xu, M. Chen, P. Guo, Z. Dai, et al., clusterProfiler 4.0: a universal enrichment tool for interpreting omics data, Innovation 2 (2021) 100141, https://doi.org/10.1016/j.xinn.2021.100141.
[25] E. Canalis, L. Schilling, J. Yu, E. Denker, NOTCH2 promotes osteoclast maturation and metabolism and modulates the transcriptome profile during osteoclastogenesis, J. Biol. Chem. 300 (2024) 105613, https://doi.org/10.1016/j.jbc.2023.105613.
[26] J. Ding, S.L. Smith, G. Orozco, A. Barton, S. Eyre, P. Martin, Characterisation of CD4 + T-cell subtypes using single cell RNA sequencing and the impact of cell number and sequencing depth, Sci. Rep. 10 (2020) 19825, https://doi.org/10.1038/s41598-020-76972-9.
[27] A. Butler, P. Hoffman, P. Smibert, E. Papalexi, R. Satija, Integrating single-cell transcriptomic data across different conditions, technologies, and species, Nat. Biotechnol. 36 (2018) 411–420, https://doi.org/10.1038/nbt.4096.
[28] T. Stuart, A. Butler, P. Hoffman, C. Hafemeister, E. Papalexi, W.M. Mauck 3rd, et al., Comprehensive integration of single-cell data, Cell 177 (2019) 1888–1902 e1821, https://doi.org/10.1016/j.cell.2019.05.031.
[29] C. Trapnell, D. Cacchiarelli, J. Grimsby, P. Pokharel, S. Li, M. Morse, et al., The dynamics and regulators of cell fate decisions are revealed by pseudotemporal ordering of single cells, Nat. Biotechnol. 32 (2014) 381–386, https://doi.org/10.1038/nbt.2859.
[30] A. Kramer, J. Green, J. Pollard Jr., S. Tugendreich, Causal analysis approaches in ingenuity pathway analysis, Bioinformatics 30 (2014) 523–530, https://doi.org/10.1093/bioinformatics/btt703.
[31] E. Canalis, Wnt signalling in osteoporosis: mechanisms and novel therapeutic approaches, Nat. Rev. Endocrinol. 9 (2013) 575–583, https://doi.org/10.1038/nrendo.2013.154, nrendo.2013.154 [pii].
[32] L. McInnes, J. Healy, J. Melville, UMAP: uniform manifold approximation and projection for dimension resolution, 2020, https://doi.org/10.48550/arXiv.1802.03426 arXiv:1802.03426v03423 [stat.ML].
[33] A.J. Roelofs, K. Kania, A.J. Rafipay, M. Sambale, S.T. Kuwahara, F.L. Collins, et al., Identification of the skeletal progenitor cells forming osteophytes in osteoarthritis, Ann. Rheum. Dis. 79 (2020) 1625–1634, https://doi.org/10.1136/annrheumdis-2020-218350.
[34] P. Mignatti, D.B. Rifkin, Nonenzymatic interactions between proteinases and the cell surface: novel roles in normal and malignant cell physiology, Adv. Cancer Res. 78 (2000) 103–157, https://doi.org/10.1016/s0065-230x(08)61024-6.
[35] A, R Kc Haseeb, M. Angelozzi, C. de Charleroy, D. Rux, R.J. Tower, et al., SOX9 keeps growth plates and articular cartilage healthy by inhibiting chondrocyte dedifferentiation/osteoblastic redifferentiation, Proc. Natl. Acad. Sci. U. S. A. 118 (2021) e2019152118, https://doi.org/10.1073/pnas.2019152118.
[36] A.N. Molin, R. Contentin, M. Angelozzi, A. Karvande, R. Kc, A. Haseeb, et al., Skeletal growth is enhanced by a shared role for SOX8 and SOX9 in promoting reserve chondrocyte commitment to columnar proliferation, Proc. Natl. Acad. Sci. U. S. A. 121 (2024) e2316969121, https://doi.org/10.1073/pnas.2316969121.
[37] J. Zieba, L. Nevarez, D. Wachtell, J.H. Martin, A. Kot, S. Wong, et al., Altered Sox9 and FGF signaling gene expression in Aga2 OI mice negatively affects linear growth, JCI Insight 8 (2023) e171984, https://doi.org/10.1172/jci.insight.171984.
[38] B.T. Martin-Marquez, F. Sandoval-Garcia, F.I. Corona-Meraz, E.A. Martinez-Garcia, P.E. Sanchez-Hernandez, M. Salazar-Paramo, et al., Osteopontin: a bone-derived protein involved in rheumatoid arthritis and osteoarthritis immunopathology, Biomolecules 13 (2023) 502, https://doi.org/10.3390/biom13030502.
[39] Y. Qu, Y. Wang, S. Wang, X. Yu, Y. He, R. Lu, et al., A comprehensive analysis of single-cell RNA transcriptome reveals unique SPP1+ chondrocytes in human osteoarthritis, Comput. Biol. Med. 160 (2023) 106926, https://doi.org/10.1016/j.compbiomed.2023.106926.
[40] A. Anwar, A.A. Zahid, K.J. Scheidegger, M. Brink, P. Delafontaine, Tumor necrosis factor-alpha regulates insulin-like growth factor-1 and insulin-like growth factor binding protein-3 expression in vascular smooth muscle, Circulation 105 (2002) 1220–1225, https://doi.org/10.1161/hc1002.105187.
[41] J.P. Thissen, J. Verniers, Inhibition by interleukin-1 beta and tumor necrosis factor-alpha of the insulin-like growth factor I messenger ribonucleic acid response to growth hormone in rat hepatocyte primary culture, Endocrinology 138 (1997) 1078–1084, https://doi.org/10.1210/endo.138.3.4966.
[42] T. Uchimura, J.M. Hollander, D.S. Nakamura, Z. Liu, C.J. Rosen, I. Georgakoudi, et al., An essential role for IGF2 in cartilage development and glucose metabolism during postnatal long bone growth, Development 144 (2017) 3533–3546, https://doi.org/10.1242/dev.155598.
[43] L.A. Bach, IGF-binding proteins, J. Mol. Endocrinol. 61 (2018) T11–T28, https://doi.org/10.1530/JME-17-0254.
[44] A. Giustina, G. Mazziotti, E. Canalis, Growth hormone, insulin-like growth factors, and the skeleton, Endocr. Rev. 29 (2008) 535–559.
[45] C. Wen, L. Xu, X. Xu, D. Wang, Y. Liang, L. Duan, Insulin-like growth factor-1 in articular cartilage repair for osteoarthritis treatment, Arthritis Res. Ther. 23 (2021) 277, https://doi.org/10.1186/s13075-021-02662-0.
[46] C. Tavera, T. Abribat, P. Reboul, S. Dore, P. Brazeau, J.P. Pelletier, et al., IGF and IGF-binding protein system in the synovial fluid of osteoarthritic and rheumatoid arthritic patients, Osteoarthritis Cartilage 4 (1996) 263–274, https://doi.org/10.1016/s1063-4584(05)80104-9.
[47] R.C. Olney, K. Tsuchiya, D.M. Wilson, M. Mohtai, W.J. Maloney, D.J. Schurman, et al., Chondrocytes from osteoarthritic cartilage have increased expression of insulin-like growth factor I (IGF-I) and IGF-binding protein-3 (IGFBP-3) and -5, but not IGF-II or IGFBP-4, J. Clin. Endocrinol. Metab. 81 (1996) 1096–1103, https://doi.org/10.1210/jcem.81.3.8772582.
[48] D.R. Clemmons, W.H. Busby Jr., A. Garmong, D.R. Schultz, D.S. Howell, R.D. Altman, et al., Inhibition of insulin-like growth factor binding protein 5 proteolysis in articular cartilage and joint fluid results in enhanced concentrations of insulin-like growth factor 1 and is associated with improved osteoarthritis, Arthritis Rheum. 46 (2002) 694–703, https://doi.org/10.1002/art.10222.
[49] F. De Ceuninck, A. Caliez, L. Dassencourt, P. Anract, P. Renard, Pharmacological disruption of insulin-like growth factor 1 binding to IGF-binding proteins restores anabolic responses in human osteoarthritic chondrocytes, Arthritis Res. Ther. 6 (2004) R393–R403, https://doi.org/10.1186/ar1201.
[50] K.D. Ham, T.R. Oegema, R.F. Loeser, C.S. Carlson, Effects of long-term estrogen replacement therapy on articular cartilage IGFBP-2, IGFBP-3, collagen and proteoglycan levels in ovariectomized cynomolgus monkeys, Osteoarthritis Cartilage 12 (2004) 160–168, https://doi.org/10.1016/j.joca.2003.08.002.